Heavy Flavor Kinematic Correlations in Cold Nuclear Matter

R. Vogt

Lawrence Livermore National Laboratory, Livermore, CA 94551, USA
Physics Department, University of California, Davis, CA 95616, USA

based on:
RV, Phys. Rev. C 98 (2018) 034907
RV, Phys. Rev. C 101 (2020) 024910

Figure 1: This work was performed under the auspices of the U.S. Department of Energy by Lawrence Livermore National Laboratory under Contract DE-AC52-07NA27344 and supported by the U.S. Department of Energy, Office of Science, Office of Nuclear Physics (Nuclear Theory) under contract number DE-SC-0004014. (LLNL-PRES-810219)

Outline

- **Heavy flavor production**
  - **fragmentation**
  - k_T **broadening**
  - **Comparison to single inclusive** p_T **data**
- **Heavy flavor pairs**
  - **Effects of fragmentation and broadening on pair production**
  - $b\bar{b} \to J/\psi J/\psi$ **comparison with data**
- **Cold nuclear matter effects**

Motivation

- **Correlations are more complex observables of heavy flavor production**
- **Naive expectation is that pairs are produced back-to-back (as at leading order) but next-to-leading order contributions change correlation**
- **Result depends more on k_T broadening than fragmentation/hadronization**
- **Correlation measurements probe event topologies by applying different kinematic cuts**
- ***a different topology does not mean a different production mechanism***
- **The presence of cold or hot nuclear matter can modify these correlations**

Production of $Q\overline{Q}$ Pairs

NLO and higher order heavy flavor production can be calculated as total cross sections (all momenta integrated away); single inclusive (keep only momentum of one quark or antiquark, momenta of other final-state partons integrated away); exclusive pair production (keep all momenta of final-state partons)

Total cross sections are generally somewhat larger: fixed flavors, α_s does not run

Single inclusive distributions: $\alpha_s(\mu_R \propto m_T)$; NLO calculations improved by resummed terms at high p_T, $p_T \gg m$ (finite heavy quark mass keeps single inclusive distribution finite at $p_T \to 0$ by subtracting massless limit) and scheme-appropriate fragmentation functions (examples: FONLL (Cacciari and Nason) and GM-VFN (Kniehl *et al.*, Helenius *et al.* calculations), employ $n_f + 1$ flavors in α_s

Exclusive pair production needed for correlations, retains all kinematic quantities, two general approaches:

- HVQMNR (Mangano, Nason and Ridolfi): no resummation, negative weight MC, incomplete numerical cancellation of divergences at $p_T \to 0$, Peterson function is default fragmentation scheme
- POWHEG-hvq (Frixione, Nason and Ridolfi): leading log resummation, positive weight MC, generally interfaces with parton shower LO MC like HERWIG or PYTHIA for fragmentation and decay

Here, HVQMNR calculates correlations with fragmentation function and k_T broadening adjusted to reproduce FONLL p_T distribution with same m_Q, μ_F and μ_R

Implementing Fragmentation

FONLL uses different fragmentation schemes for charm and bottom

bottom quarks: Polynomial

$$D(z) = z(1-z)^{\epsilon}$$

$\epsilon = 27.5$ **for** $m_b = 4.65$ **GeV,** $\langle z \rangle = 0.934$

HVQMNR employs Peterson function for fragmentation with parameter ϵ_P **for both charm and bottom,**

$$D(z) = \frac{z(1-z)^2}{((1-z)^2 + z\epsilon_P)^2}$$

- **Standard value of** ϵ_P**, 0.006 for bottom, too large for hadroproduction,** $\langle z \rangle = 0.82$
- **To match the FONLL result at high** p_T**, with** k_T **broadening,** ϵ_P **needs to be reduced to 0.0004 for** b **quarks, resulting in** $\langle z \rangle = 0.930$

Fragmentation Functions

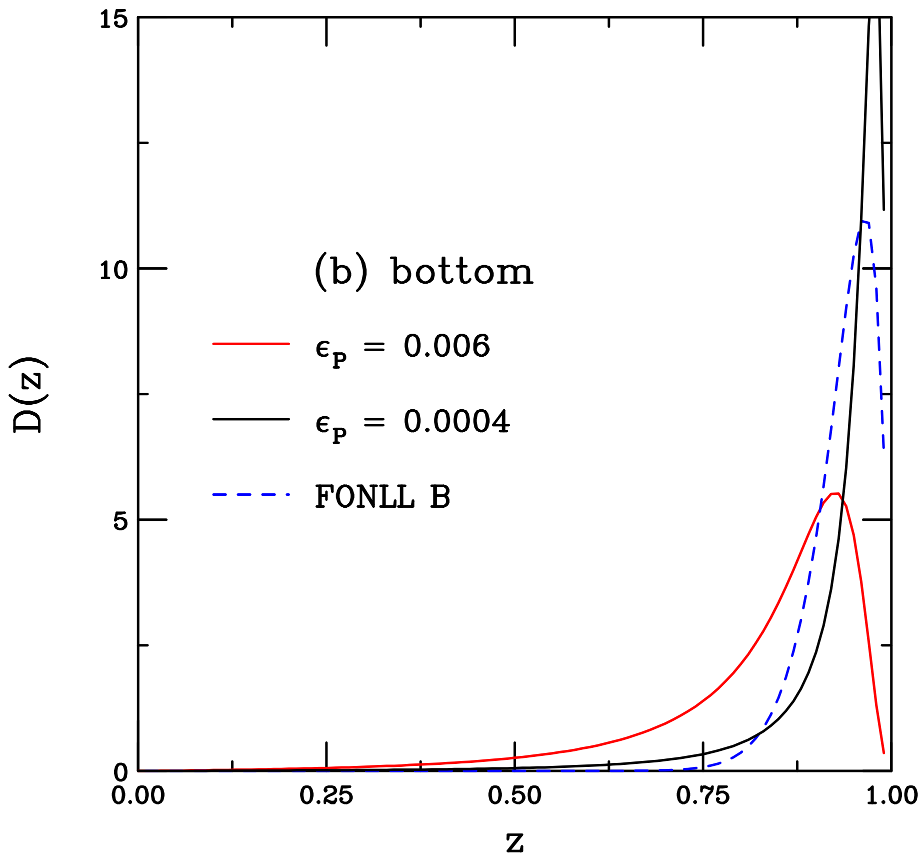

Figure 2: **The fragmentation functions used in the HVQMNR code and FONLL for bottom are compared. The red curves show the standard Peterson function parameter while the black curves are calculated with the values of ϵ_P used in this paper. The FONLL results are shown in the dashed blue curves.**

Implementation of k_T Broadening

FONLL only includes fragmentation, not broadening

Default HVQMNR combines broadening with fragmentation based on p_T distributions at fixed-target energies: including standard Peterson ϵ_P reduced average p_T at fixed-target energies considerably; rather large k_T broadening had to be included to make up difference and match data

Precedent from Drell-Yan, k_T broadening included to make low p_T distribution finite and take the place of full resummation

$$g(k_T) = \frac{1}{\pi \langle k_T^2 \rangle} \exp(-k_T^2/\langle k_T^2 \rangle)$$

In HVQMNR Gaussian factors are applied to each heavy quark in the final state, should be equivalent to application to initial-state partons as long as $\langle k_T^2 \rangle \sim 2 - 3$ GeV^2

Energy dependence of broadening assumed,

$$k_T^2 = 1 + \frac{1}{n} \ln \left(\frac{\sqrt{s}}{20\,\mathrm{GeV}} \right) \ \mathrm{GeV}^2$$

n **fixed from Υ p_T distributions,** $n = 3$

Fragmentation and Broadening Effects on Single Inclusive p_T Distributions

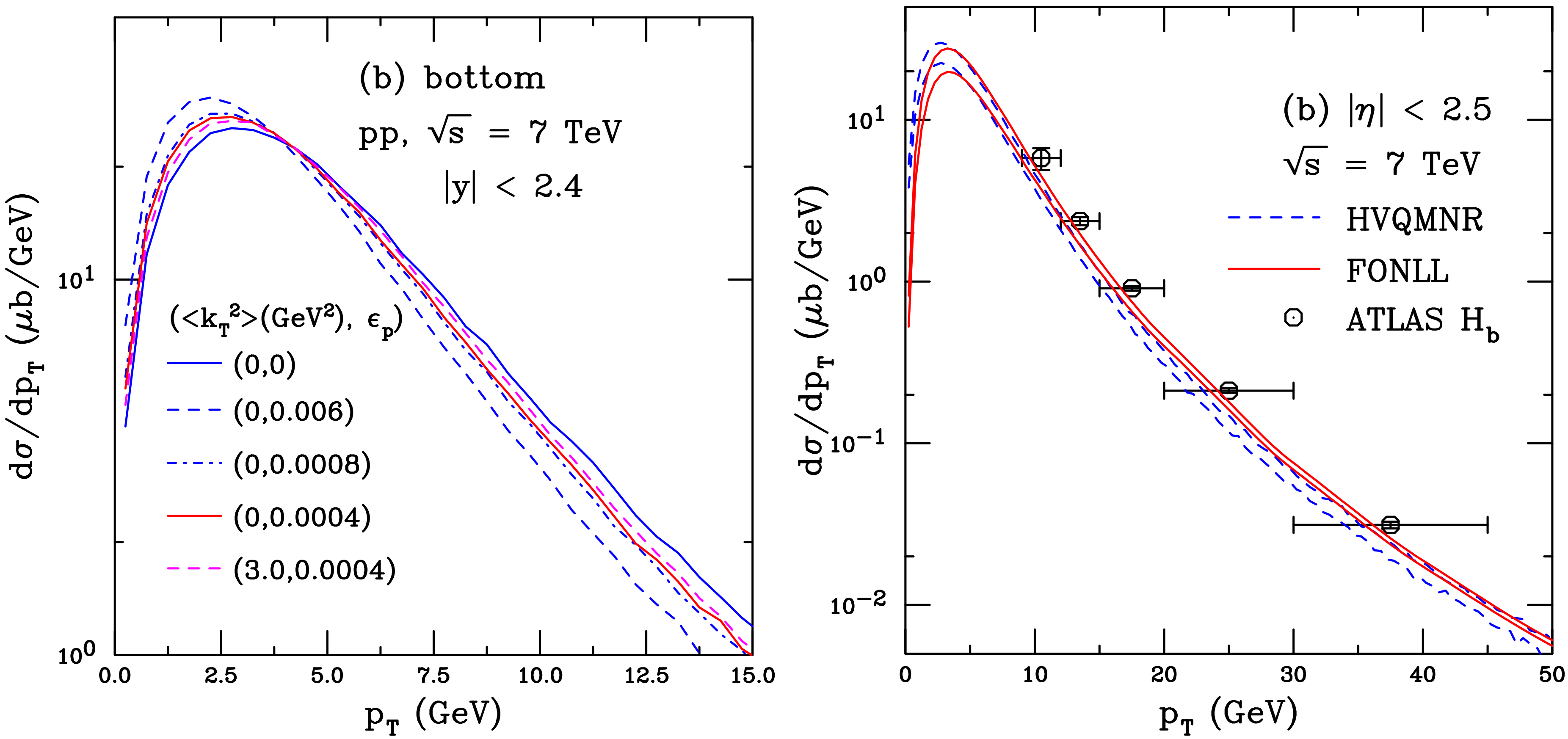

Figure 3: **(Left) The single inclusive bottom quark distributions in $\sqrt{s} = 7$ TeV $p + p$ collisions at next-to-leading order using the HVQMNR code. The distributions are shown at midrapidity, $|y| < 2.4$. Results are given for various combinations of $\langle k_T^2 \rangle$ and ϵ_P. (Right) The single inclusive b-quark hadron, H_b, distributions in $\sqrt{s} = 7$ TeV $p + p$ collisions are compared to data from ATLAS (G. Aad *et al.* [ATLAS Collaboration], Nucl. Phys. B 864, 341 (2012)) at $|\eta| < 2.5$ respectively. The curves show the extent of the theoretical uncertainty bands. The HVQMNR code (blue dashed curves) utilizes $(\langle k_T^2 \rangle(\mathrm{GeV}^2), \epsilon_P) = (1.5, 0.008)$ for charm and (3,0.0004) for bottom. The corresponding FONLL uncertainty band (red curves) is also shown. The same quark mass and scale parameters are used in both calculations.**

Fragmentation and Broadening Effects on Azimuthal Angle Difference Between Heavy Quarks

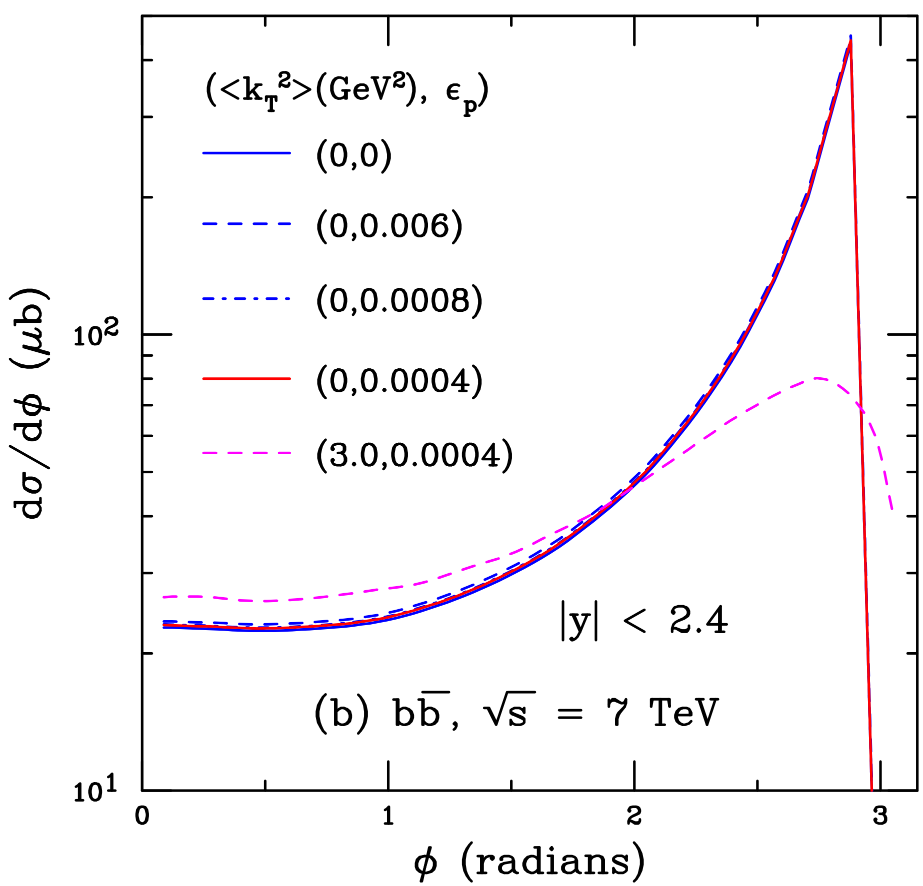

Figure 4: **The NLO azimuthal distribution between two heavy quarks, $d\sigma/d\phi$ in $p+p$ collisions at $\sqrt{s} = 7$ TeV using the HVQMNR code for $b\bar{b}$ pairs at midrapidity, $|y| < 2.4$. The results are shown for various choices of $\langle k_T^2 \rangle$ and ϵ_P.**

Dependence of Azimuthal Correlations on $\langle k_T^2 \rangle$

Studied sensitivity of azimuthal correlations on $\langle k_T^2 \rangle$ and p_T cut

$$k_T^2 = 1 + \frac{\Delta}{n} \ln \left(\frac{\sqrt{s}}{20\,\mathrm{GeV}} \right) \ \mathrm{GeV}^2$$

Studied $\Delta = -1/2, 0, 1/2, 1$

Low p_T is most sensitive to k_T in azimuthal correlation, as is now shown

Effect is independent of rapidity

Bottom Pairs, $p_T < 10$ GeV

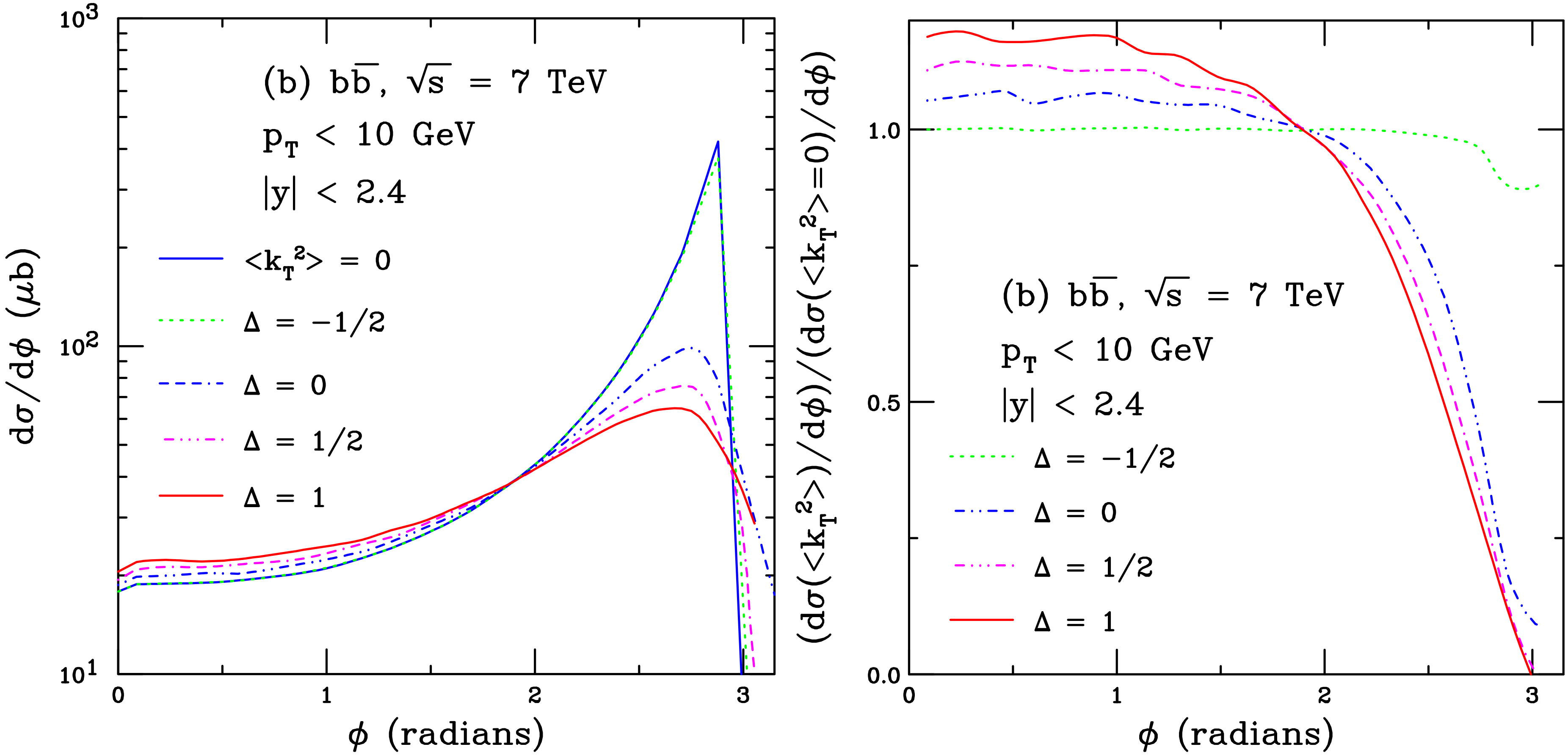

Figure 5: **The azimuthal angle distributions (left) and ratios relative to $\langle k_T^2 \rangle = 0$ (right) for $b\bar{b}$ in the central rapidity range $|y| < 2.4$ with $p_T < 10$ GeV. Calculations are shown with $\langle k_T^2 \rangle = 0$ and for values of Δ from $-1/2$ to 1.**

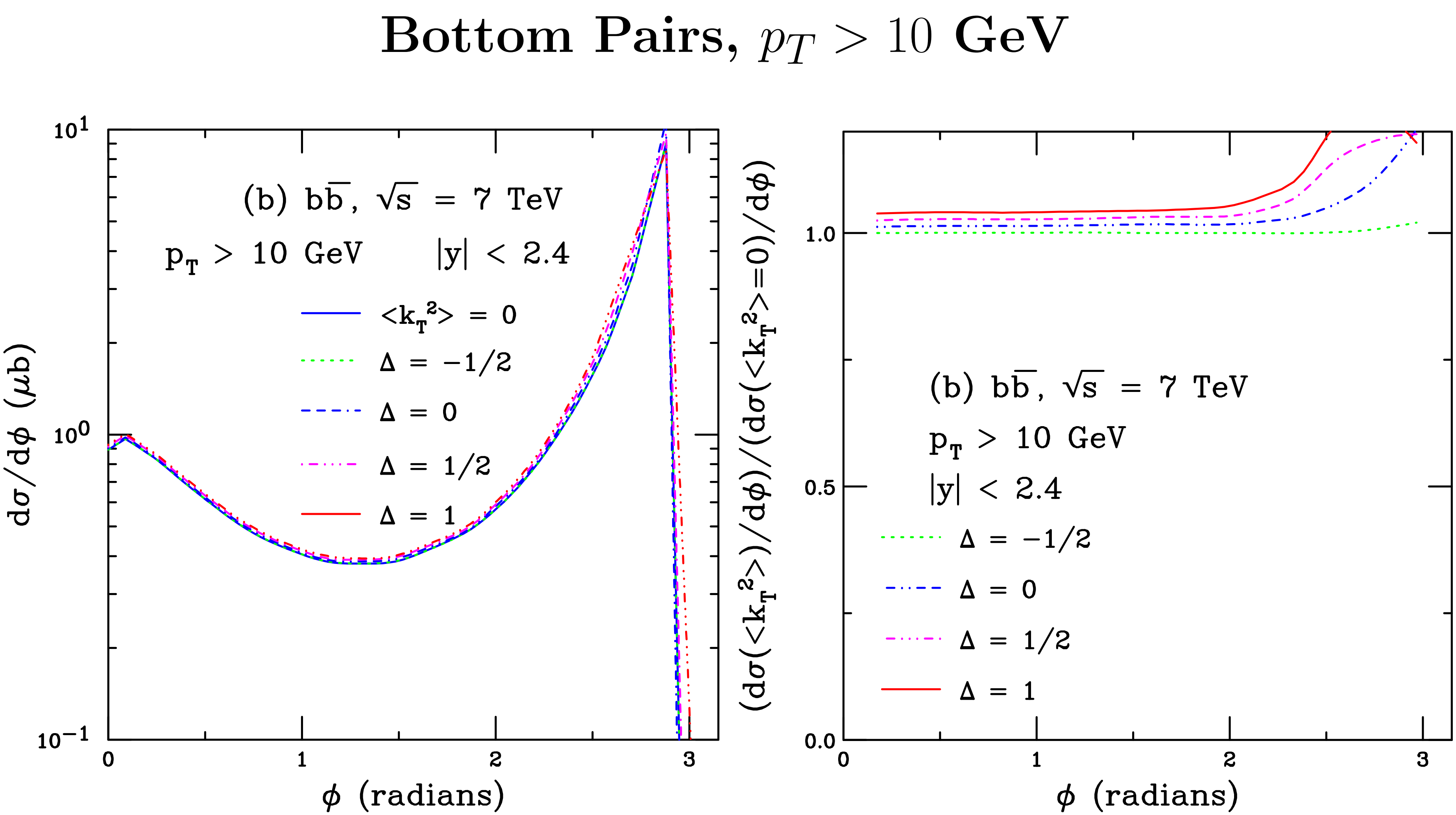

Figure 6: **The azimuthal angle distributions (left) and ratios relative to $\langle k_T^2 \rangle = 0$ (right) for $b\bar{b}$ in the central rapidity range $|y| < 2.4$ with $p_T > 10$ GeV. Calculations are shown with $\langle k_T^2 \rangle = 0$ and for values of Δ from $-1/2$ to 1.**

LHC $b\bar{b} \to J/\psi J/\psi$ Correlations

LHCb measured $b\bar{b} \to J/\psi J/\psi$ at $\sqrt{s} = 7$ and 8 TeV (R. Aaij *et al.* (LHCb Collaboration), JEHP 11 (2017) 030)

Presented results for six pair observables:

- **$|\Delta\phi^*|$, the difference in azimuthal angle between the b and $\bar{b}$ mesons, also $|\Delta\phi|$, the azimuthal opening angle between the two J/ψs**
- **$|\Delta\eta^*|$, the difference in pseudorapidity between the b and $\bar{b}$ mesons and $|\Delta\eta|$ between the two J/ψs**
- **A_T, the asymmetry between the transverse momenta of the J/ψs**
- **Mass, M, of the J/ψ pair**
- **J/ψ pair transverse momentum, p_{T_p}**
- **J/ψ pair rapidity, y_p**

Each observable was studied with four different p_T cuts: $p_T > 2$, 3, 5 and 7 GeV

All the pair observables studied by LHCb will be calculated for both the parent $b\bar{b}$ mesons and the subsequent $J/\psi J/\psi$ decays.

Azimuthal Distributions, $|\Delta\phi^*|$ and $|\Delta\phi|$

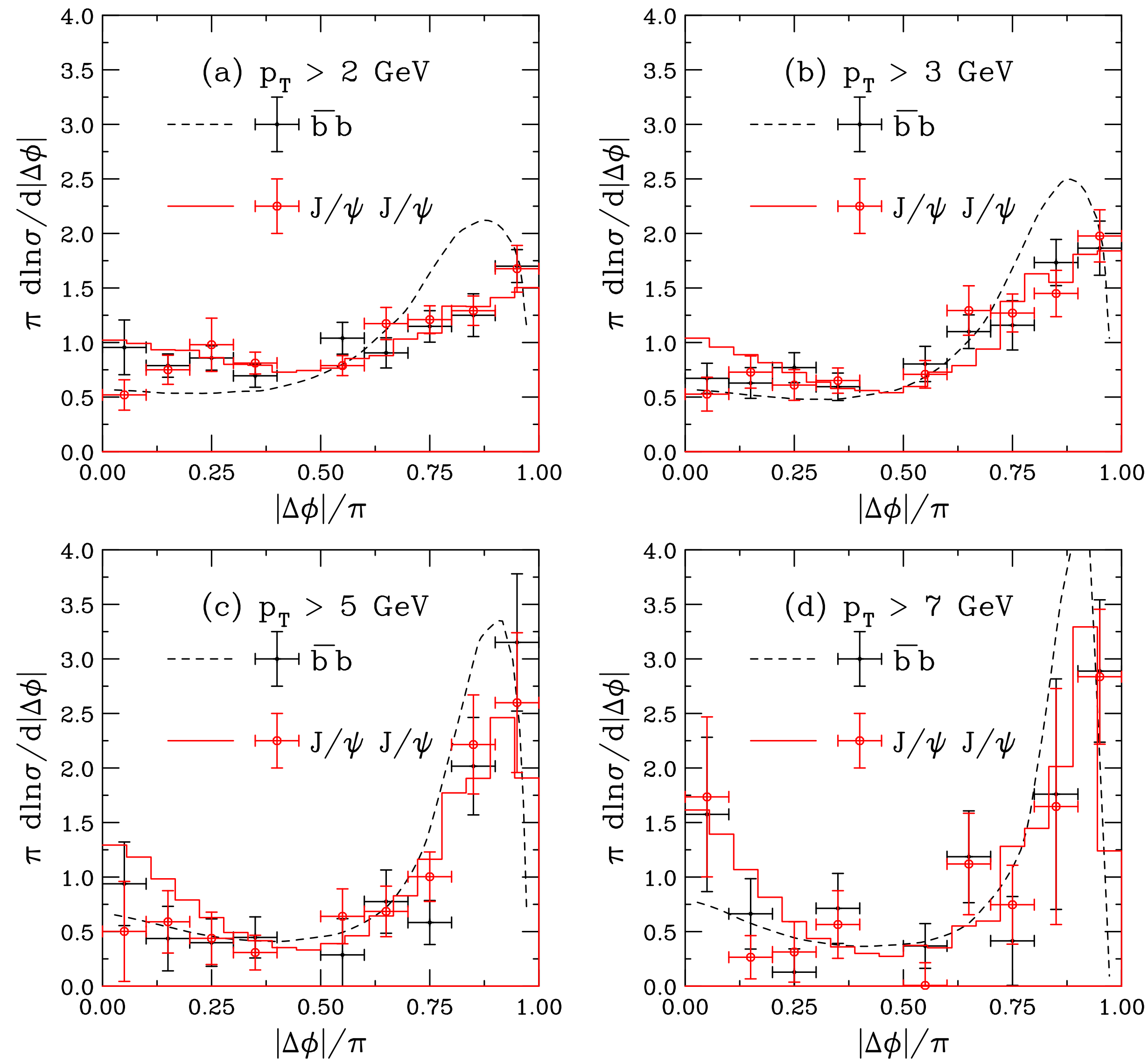

Figure 7: **The azimuthal angle difference between the b and $\bar{b}$ (black dashed curves) and the J/ψ's resulting from B decays (red histograms) are compared to the LHCb data (black: $b\bar{b}$, red circles: J/ψ pairs) for p_T cuts on the B and the J/ψ of 2 (a), 3 (b), 5 (c) and 7 GeV (d).**

Rapidity Difference, $|\Delta y^*|$ and $|\Delta y|$

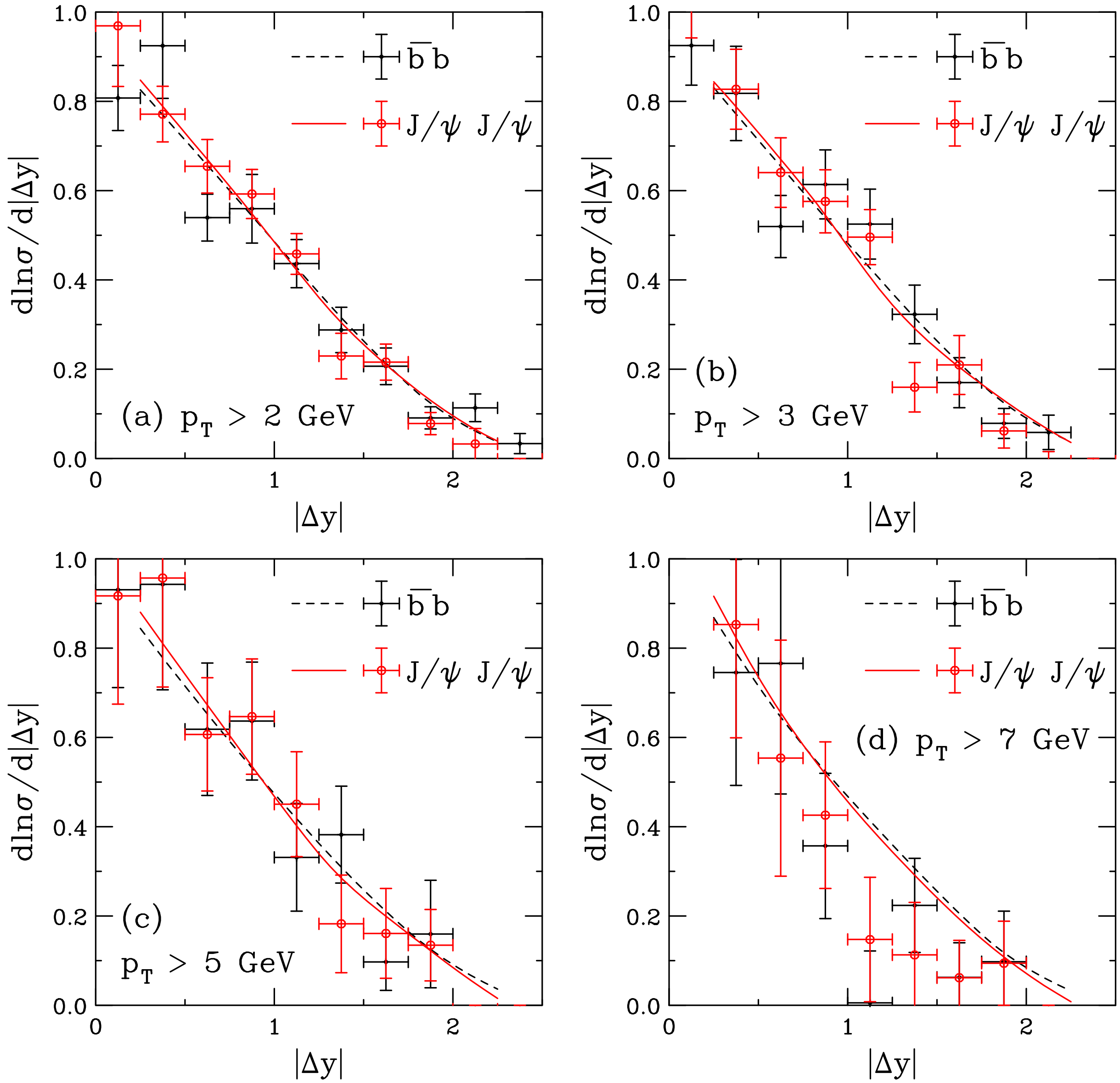

Figure 8: **The rapidity difference $|\Delta y|$ between the b and $\bar{b}$ (black dashed curve) and the J/ψ's resulting from B decays (red solid curve) are compared to the LHCb data (black: $b\bar{b}$, red circles: J/ψ pairs) for p_T cuts on the B and the J/ψ of 2 (a), 3 (b), 5 (c) and 7 GeV (d).**

p_T Asymmetry $A_T = |(p_{T_1} - p_{T_2})/(p_{T_1} + p_{T_2})|$

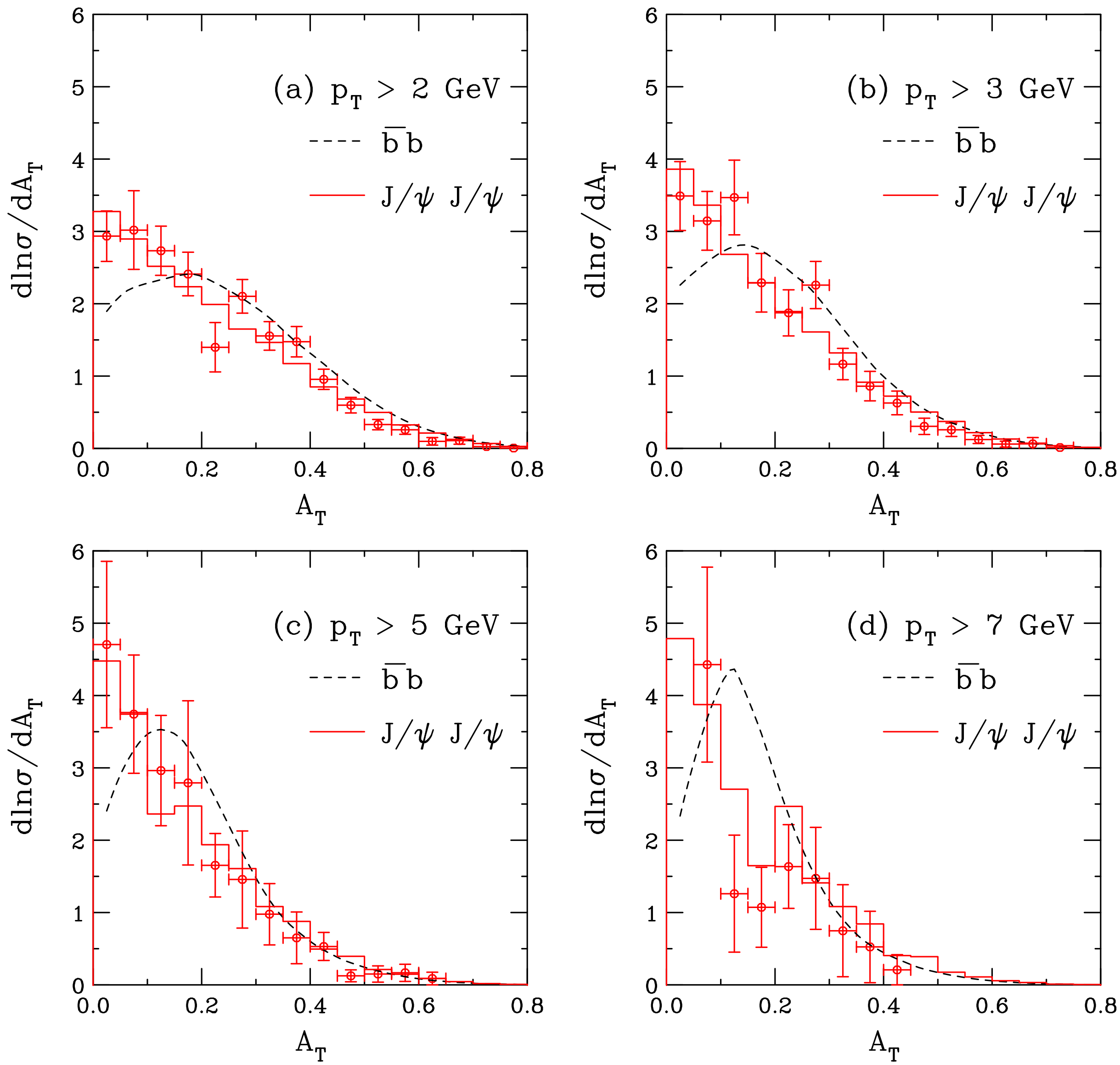

Figure 9: **The p_T asymmetry between the b and $\bar{b}$ (black dashed lines) and the J/ψ's resulting from B decays (red histograms) are compared to the LHCb data (red circles) for p_T cuts on the B and the J/ψ of 2 (a), 3 (b), 5 (c) and 7 GeV (d).**

Pair p_{T_p} Distributions

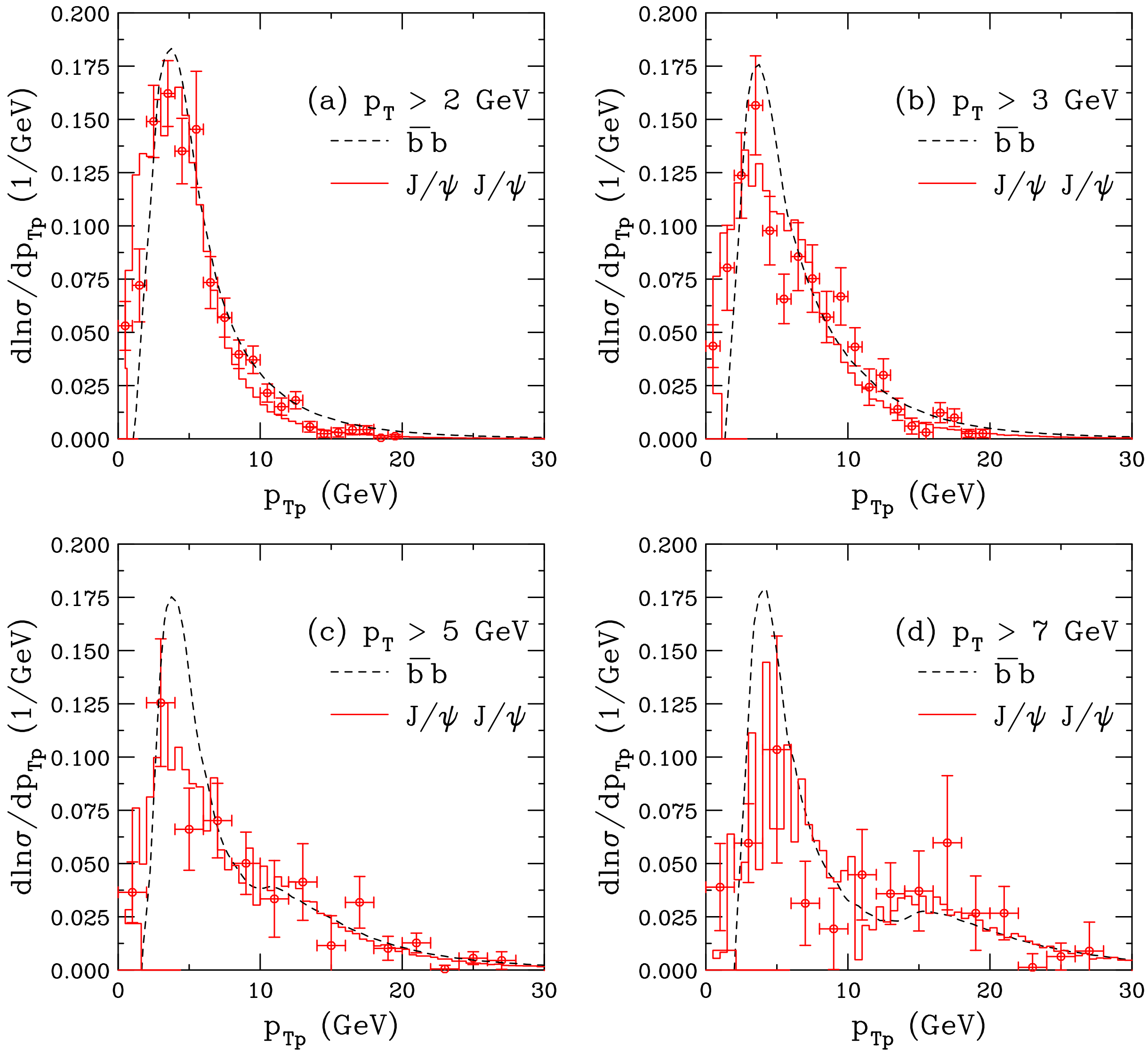

Figure 10: **The transverse momentum of the b and $\bar{b}$ (black dashed lines) and the J/ψ's resulting from B decays (red histograms) are shown compared to the LHCb data (red circles) for the p_T cuts on the B and the J/ψ of 2 (a), 3 (b), 5 (c) and 7 GeV (d).**

Pair Mass Distributions, M

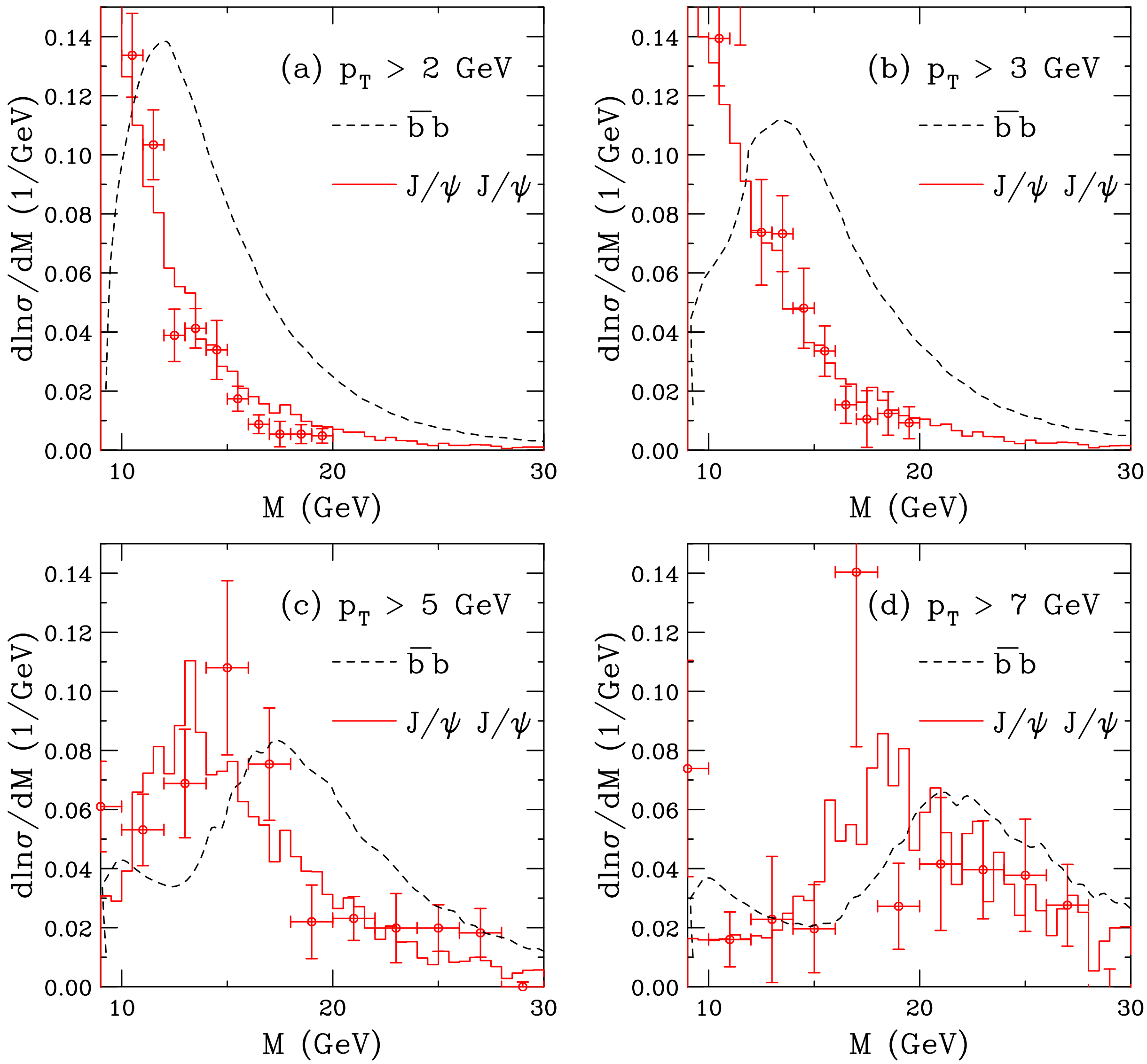

Figure 11: **The pair mass of the b and $\bar{b}$ (black dashed lines) and the J/ψ's resulting from B (red histograms) are compared to the LHCb data (red circles) for p_T cuts on the B and the J/ψ of 2 (a), 3 (b), 5 (c) and 7 GeV (d).**

Pair Rapidity Distributions, y_p

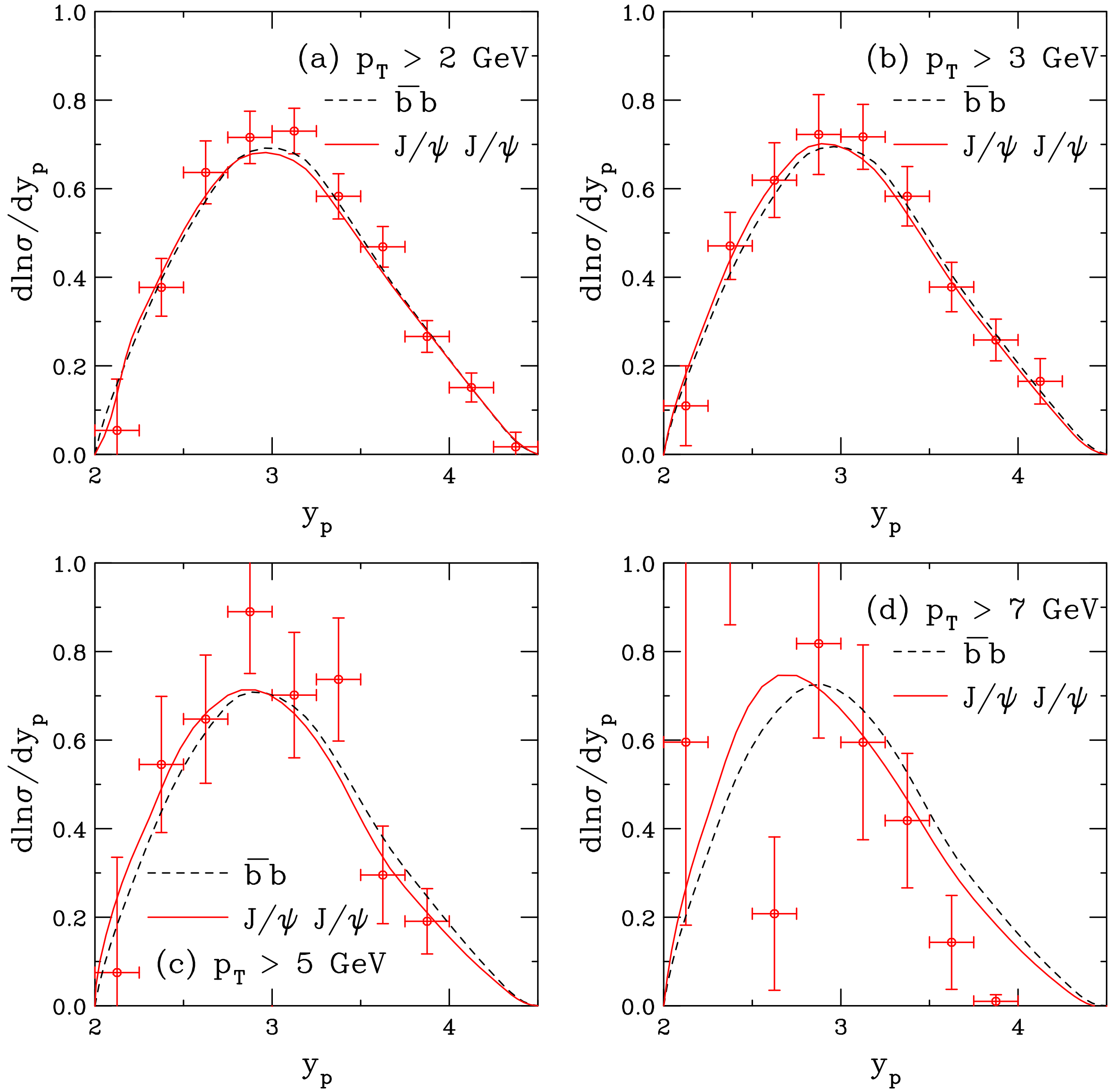

Figure 12: **The pair rapidity of the b and $\bar{b}$ (black dashed curves) and the J/ψ's resulting from B decays (red solid curves) are compared to the LHCb data (red circles) for p_T cuts on the B and the J/ψ of 2 (a), 3 (b), 5 (c) and 7 GeV (d).**

Sensitivity to $\langle k_T^2 \rangle$

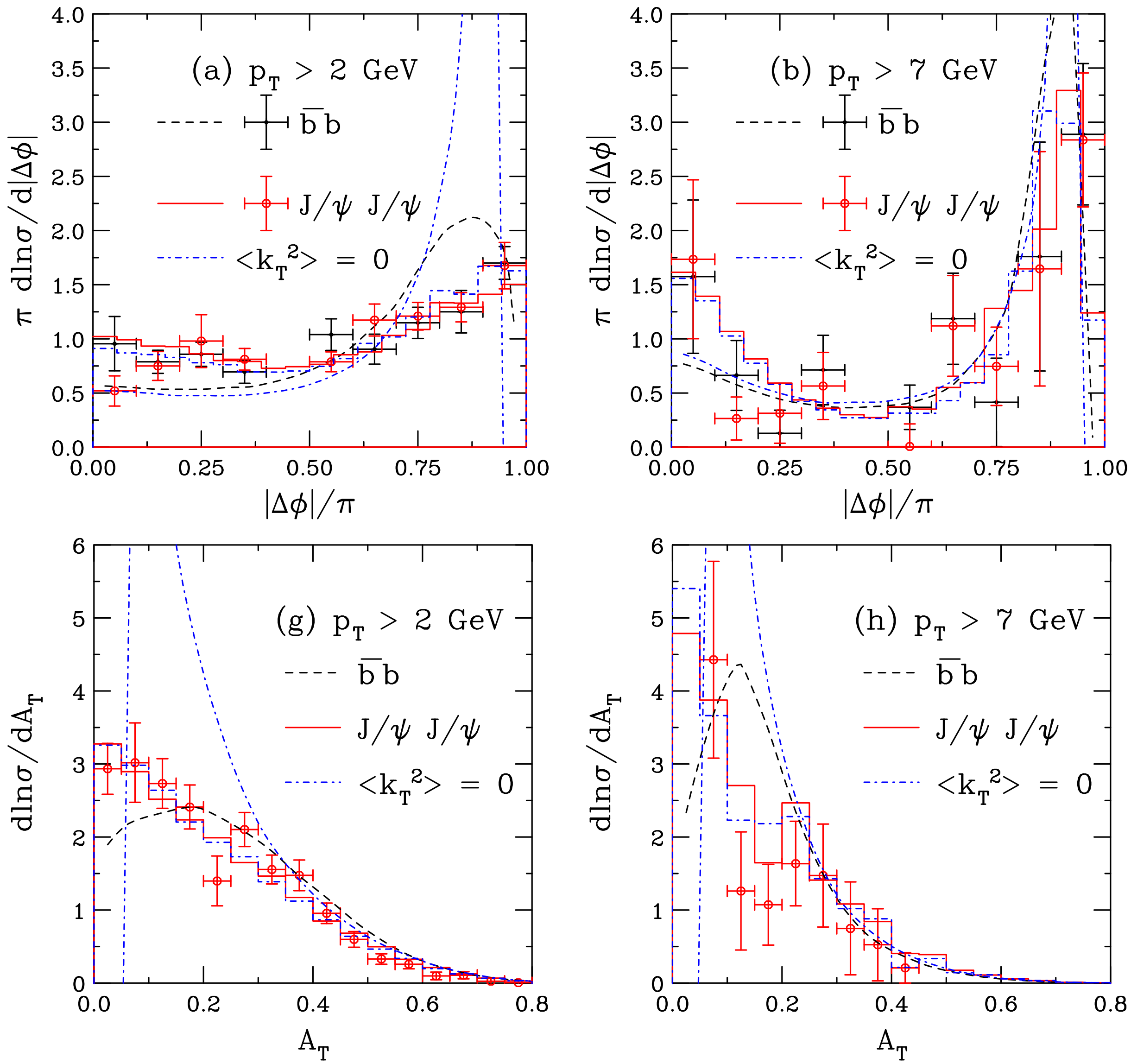

Figure 13: **The difference in the $b\bar{b}$ and $J/psiJ/\psi$ pair results for $\langle k_T^2 \rangle = 0$ and the default k_T kick. The $\langle k_T^2 \rangle = 0$ results are shown by the blue dot-dashed curves ($b\bar{b}$) and blue dot-dashed histograms ($J/\psi J/\psi$) and with the default k_T kick by the black dashed curves ($b\bar{b}$) and red histograms ($J/\psi J/\psi$). Results are shown for the azimuthal angle difference (a) and (b) and p_T asymmetry (g) and (h).**

Nuclear Matter Effects

Cold nuclear matter effects include modification of the parton densities, energy loss and p_T broadening (Cronin effect), last two are also hot matter effects

Usually defined in terms of nuclear modification factors, per nucleon cross sections in pA or AA collisions relative to pp

$$R_{pA} = \frac{1}{T_A}\frac{d\sigma_{pA}/dp_T dy}{d\sigma_{pp}/dp_T dy} \quad R_{AA} = \frac{1}{T_{AA}}\frac{d\sigma_{AA}/dp_T dy}{d\sigma_{pp}/dp_T dy}$$

Nuclear modification of parton densities (shadowing) changes parton distributions in the nucleus: $f_i^A(x,Q^2) = S_i^A(x,Q^2) f_i^p(x,Q^2)$ where f_i is the parton density ($i = q$, $\overline{q}$ or g) and S_i^A is the shadowing factor, determined from global analyses

Cronin effect modeled by enhanced k_T broadening in the nucleus:

$$k_T^2 = 1 + \frac{\Delta}{n}\ln\left(\frac{\sqrt{s}}{20\,\mathrm{GeV}}\right)\ \mathrm{GeV}^2 \quad [pA : \Delta = 2, \ \ AA : \Delta = 4]$$

Energy loss modeled by assuming that the fragmentation parameter is increased, to do so ϵ_P is taken to be the e^+e^- value in AA collisions

Single Hadron p_T Distributions and Pair Observables

Several scenarios are studied for bottom production:

- **Nuclear modification of parton densities (shadowing) only in** pA **and** AA
- **Shadowing plus additional broadening** ($\Delta = 2$) **in** pA
- **Shadowing, additional broadening** ($\Delta = 4$)**, and increased** ϵ_P **in** AA
- pA **calculated at** $\sqrt{s_{NN}} = 8.16$ **TeV;** AA **at** $\sqrt{s_{NN}} = 5.02$ **TeV;** pp **calculated at the same energies**
- **Results shown only for forward rapidities, similar dependence at central rapidity, see paper for more details**
- **Studied pair quantities** $|\Delta\phi|$ **and** y_p

The results for pair rapidities are more sensitive to changes in fragmentation while azimuthal effects are more sensitive to enhanced k_T **broadening**

Sensitivity to transverse momentum studied by employing the same p_T **cuts as LHCb** $b\bar{b} \to J/\psi J/\psi$ **studies,** B $p_T > 2$**, 3, 5 and 7 GeV**

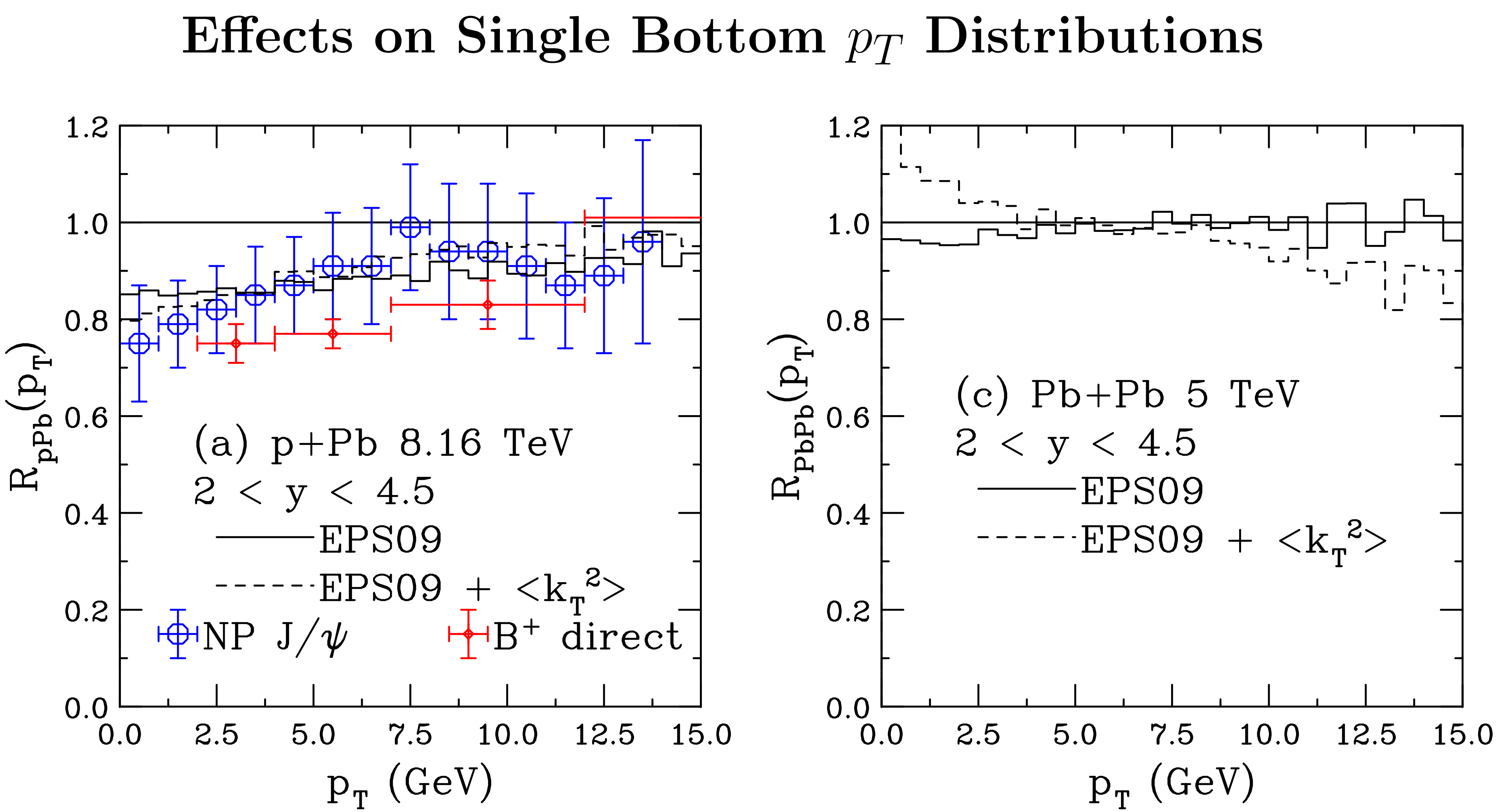

Figure 14: **Cold nuclear matter effects on b quark p_T distributions for (a) p+Pb collisions at 8.16 TeV with central EPS09 and the same k_T kick as in $p+p$ (solid) and additional k_T broadening in Pb (dashed); (c) Pb+Pb collisions at 5 TeV with central EPS09 with the same k_T kick in $p+p$ and Pb+Pb (solid) and additional k_T broadening in the Pb nuclei with a modified fragmentation function in Pb (dashed). In (a) the calculations are compared to the LHCb data on non-prompt J/ψs (R. Aaij *et al.* [LHCb Collaboration], Phys. Lett. B 774, 159 (2017).) and direct B^+ (R. Aaij *et al.* [LHCb Collaboration], Phys. Rev. D 99, 052011 (2019).).**

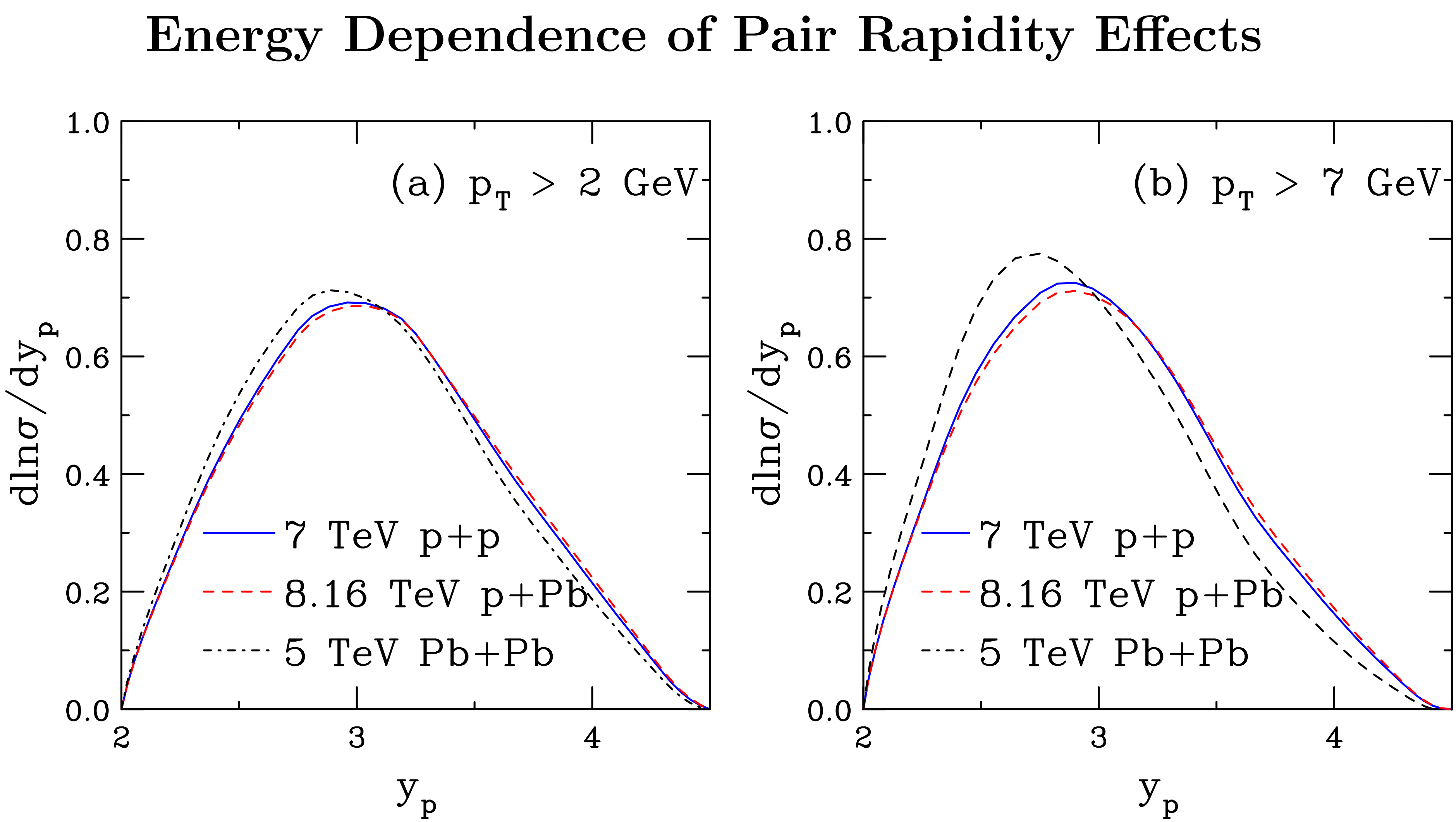

Figure 15: **The $b\bar{b}$ pair rapidity in the range $2 < y_p < 4.5$ for $p_T > 2$ (a) and 7 GeV (b) for $p + p$ collisions at 7 TeV (solid blue), p+Pb collisions at 8.16 TeV (dashed red) and Pb+Pb collisions at 5 TeV (dot-dashed black). The p+Pb calculations include shadowing and enhanced broadening (2Δ) while the Pb+Pb calculations include shadowing, broadening (4Δ), and fragmentation function modification.**

Effects on Pair Rapidity Distributions

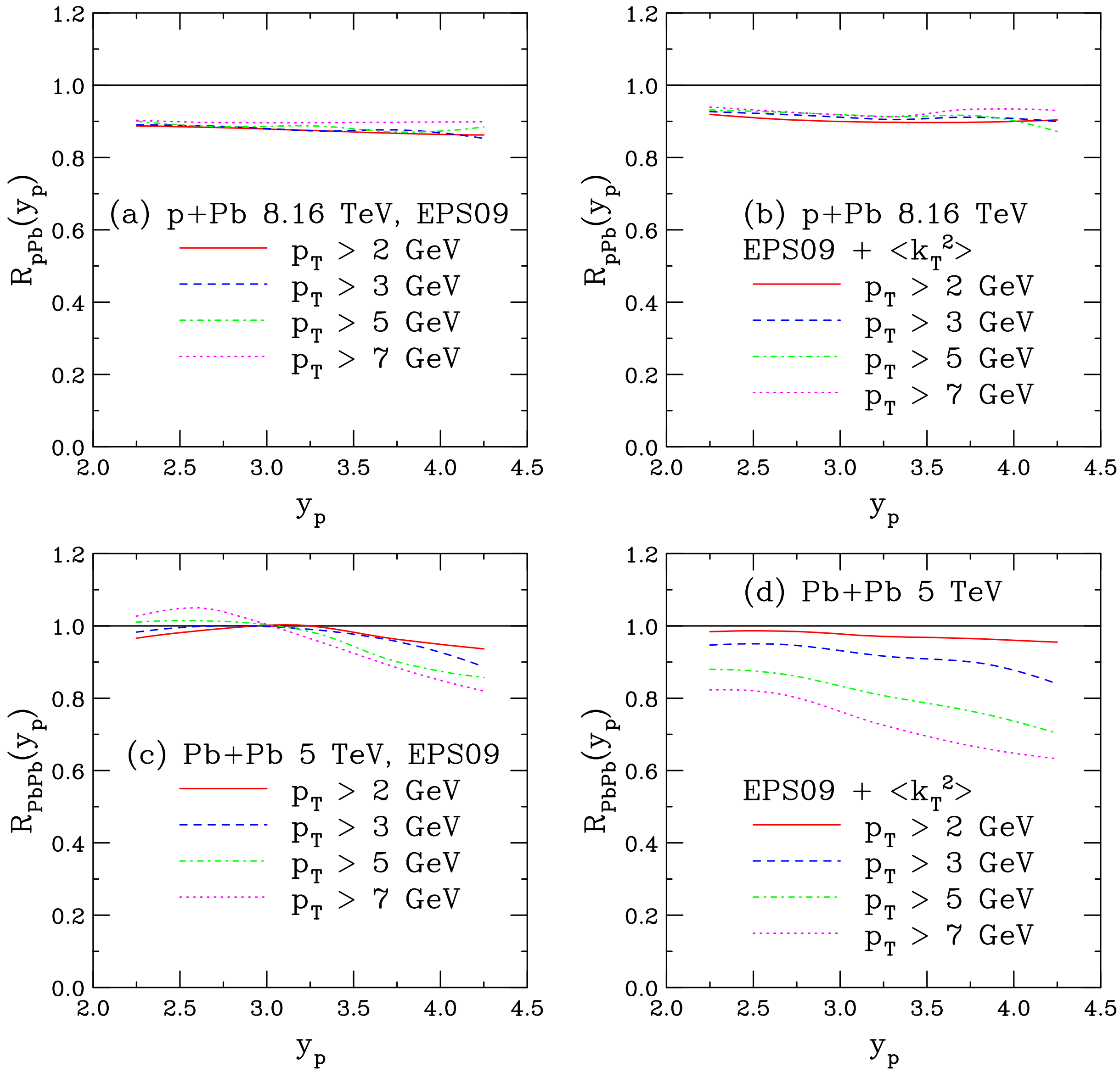

Figure 16: **Cold nuclear matter effects in $2 < y < 4.5$ on the $b\bar{b}$ pair rapidity for $p_T > 2$ (solid red), 3 (dashed blue), 5 (dot-dashed green), and 7 GeV (dotted magenta) for (a) p+Pb collisions at 8.16 TeV with central EPS09 and the same k_T kick as in $p+p$; (b) $R_{p\mathrm{Pb}}$ at 8.16 TeV with EPS09 and additional k_T broadening in Pb; (c) Pb+Pb collisions at 5 TeV with central EPS09 with the same k_T kick in $p+p$ and p+Pb; and (d) R_{AA} at 5 TeV with EPS09, additional k_T broadening in the Pb nuclei, and a modified fragmentation function in Pb.**

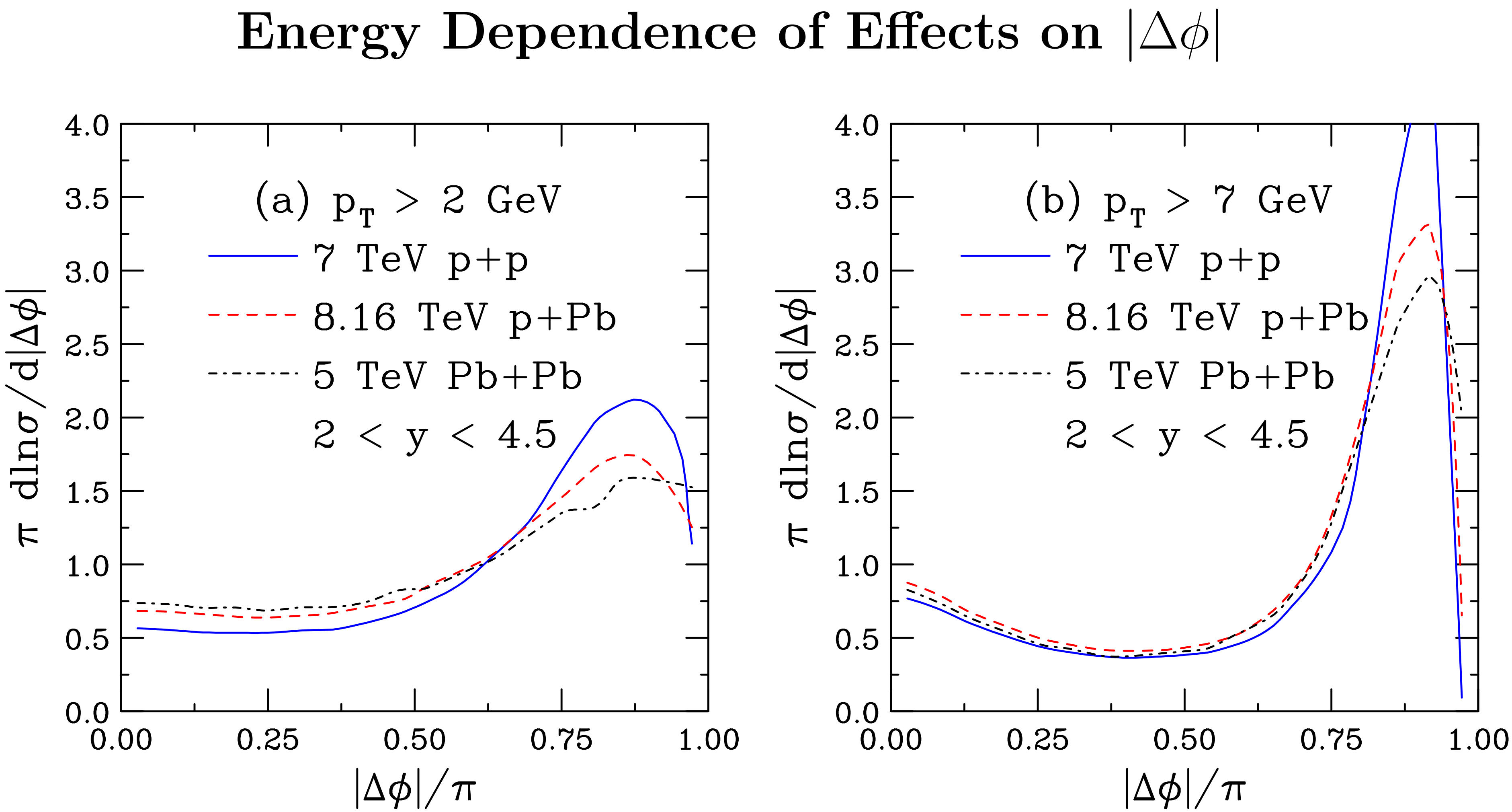

Figure 17: **The $b\bar{b}$ azimuthal difference in the range $2 < y_p < 4.5$ for $p_T > 2$ (a) and 7 GeV (b) for $p+p$ collisions at 7 TeV (solid blue), p+Pb collisions at 8.16 TeV (dashed red) and Pb+Pb collisions at 5 TeV (dot-dashed black). The p+Pb calculations include shadowing and enhanced broadening (2Δ) while the Pb+Pb calculations include shadowing, broadening (4Δ), and fragmentation function modification.**

Effects on Azimuthal Distributions

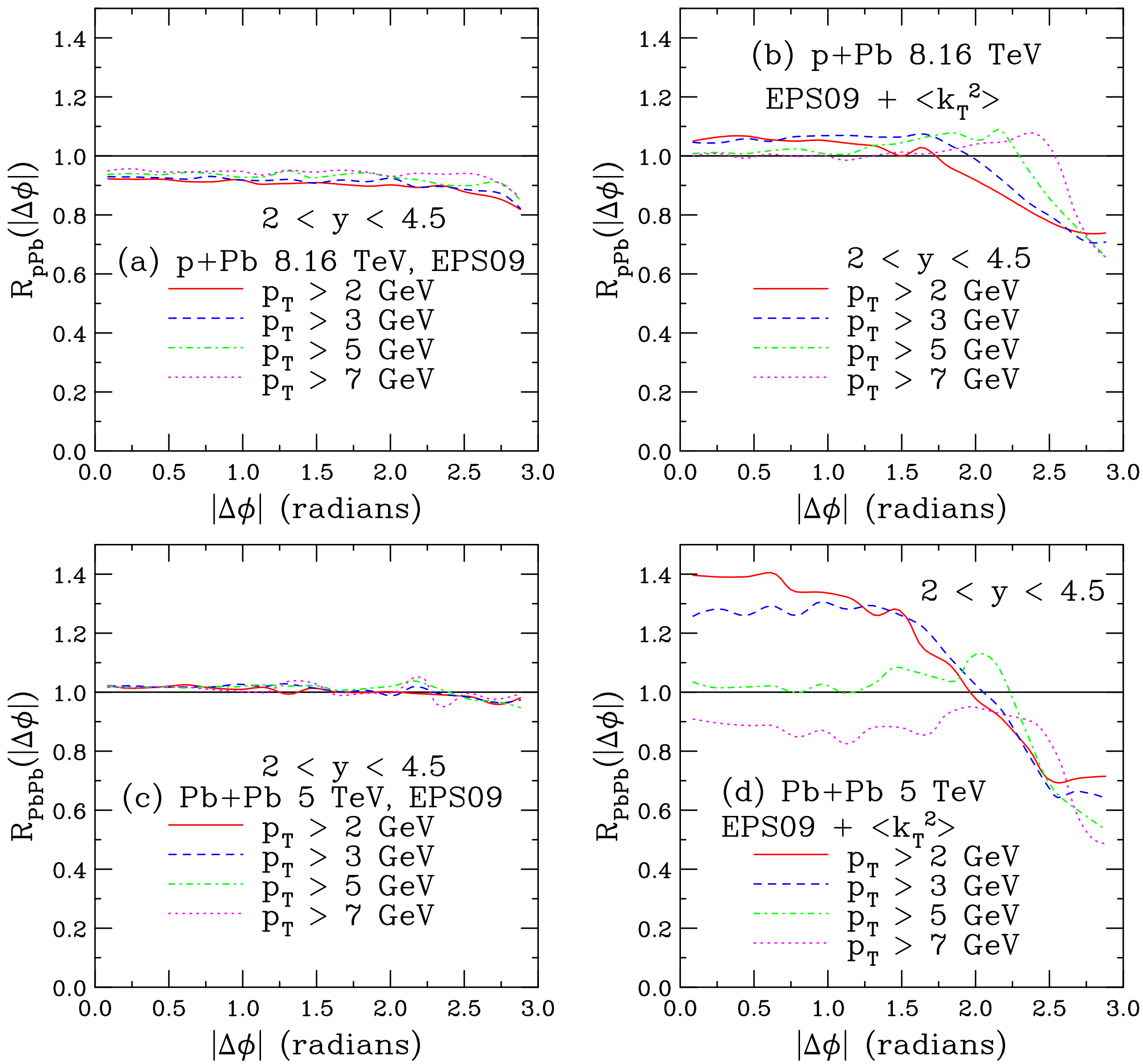

Figure 18: **Cold nuclear matter effects at forward rapidity ($2 < y < 4.5$) on the $b\bar{b}$ azimuthal angle difference for $p_T > 2$ (solid red), 3 (dashed blue), 5 (dot-dashed green), and 7 GeV (dotted magenta) for (a) p+Pb collisions at 8.16 TeV with central EPS09 and the same k_T kick as in $p+p$; (b) $R_{p\mathrm{Pb}}$ at 8.16 TeV with EPS09 and additional k_T broadening in Pb; (c) Pb+Pb collisions at 5 TeV with central EPS09 with the same k_T kick in $p+p$ and p+Pb; and (d) R_{AA} at 5 TeV with EPS09, additional k_T broadening in the Pb nuclei and a modified fragmentation function in Pb.**

Summary

- **Heavy quark pair correlations in $p+p$ and $p\overline{p}$ collisions can be explained by NLO heavy flavor production processes**
- **Results are most sensitive to k_T broadening at low p_T, practically insensitive to fragmentation/hadronization**
- **All $b\overline{b} \rightarrow J/\psi J/\psi$ observables are in good agreement with NLO $b\overline{b}$ pair production and decay to J/ψ**
- **$b\overline{b}$ pair quantities sensitive to k_T effects but daughter J/ψs are not because the decay results in de-correlation of k_T**
- **Effects on pair observables sensitive to hot and cold nuclear matter effects; results here are illustrative only but show that pair rapidity can be sensitive to energy loss while azimuthal angle difference is sensitive to Cronin-like p_T broadening effects**

Contributions to $Q\overline{Q}$ Pair Production

Only gg and $q\overline{q}$ at LO, at NLO there is new channel, $q(\overline{q})g$

Contributions sorted by initial state, not diagram topology as in LO event generators with labels like flavor creation, flavor excitation and gluon splitting

These labels are for topologies, not production mechanisms, and are properly weighted in a NLO calculation by color factors, then initial state contributions are summed and amplitudes squared, not possible in event generators

Squaring amplitudes of individual diagrams, as in LO generators, eliminates interferences and will not produce correct cross sections

Some experiments use LO event generators and try to model data by fitting individual diagram weights, this is wrong

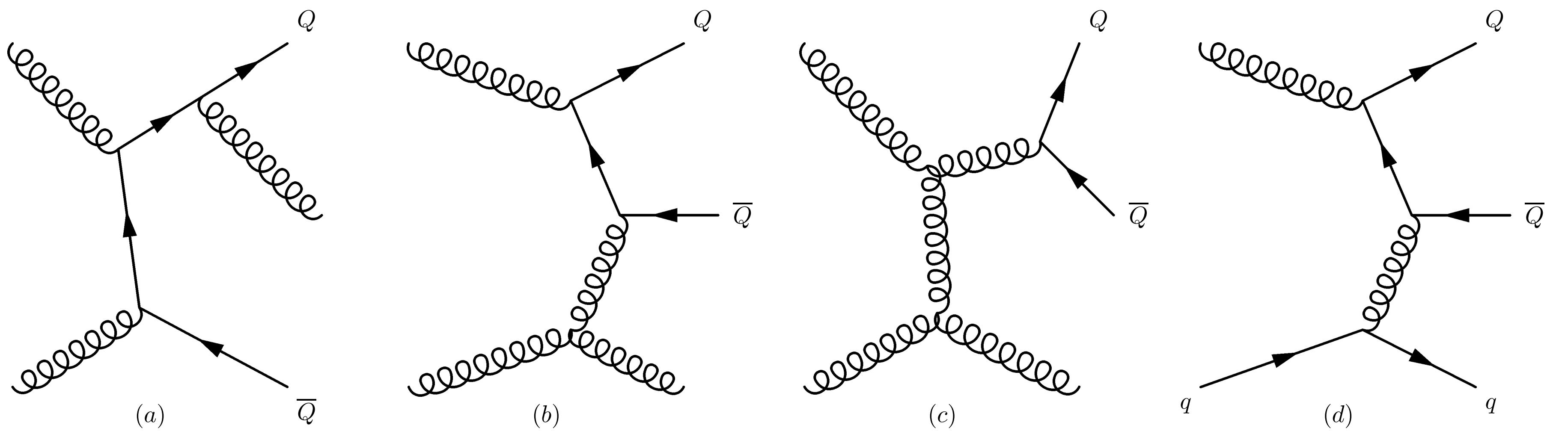

Figure 19: Examples of real contributions to next-to-leading order $Q\overline{Q}$ production. Diagrams (a)-(c) illustrate contributions to $gg \to Q\overline{Q}g$ while (d) shows an example of $qg \to qQ\overline{Q}$ production.

Calculating Theoretical Uncertainties

Scales fit to total heavy flavor cross section data

- **Take** $1S$ **value for** m_b, 4.65 ± 0.09 **GeV**
- **Vary scales independently within** 1σ **of fitted region:** $(\mu_F/m, \mu_R/m) =$ **(C,C), (H,H), (L,L), (H,C), (C,H), (L,C), (C,L)**
- **For bottom production,** $(\mu_F/m_T, \mu_R/m_T) = (1.4^{+0.77}_{-0.49}, 1.1^{+0.22}_{-0.20})$

The uncertainty band in all cases comes from the upper and lower limits of mass and scale uncertainties added in quadrature

$$\frac{d\sigma_{\rm max}}{dX} = \frac{d\sigma_{\rm cent}}{dX} + \sqrt{\left(\frac{d\sigma_{\mu,{\rm max}}}{dX} - \frac{d\sigma_{\rm cent}}{dX}\right)^2 + \left(\frac{d\sigma_{m,{\rm max}}}{dX} - \frac{d\sigma_{\rm cent}}{dX}\right)^2} \, ,$$

$$\frac{d\sigma_{\rm min}}{dX} = \frac{d\sigma_{\rm cent}}{dX} - \sqrt{\left(\frac{d\sigma_{\mu,{\rm min}}}{dX} - \frac{d\sigma_{\rm cent}}{dX}\right)^2 + \left(\frac{d\sigma_{m,{\rm min}}}{dX} - \frac{d\sigma_{\rm cent}}{dX}\right)^2} \, ,$$

The resulting theoretical uncertainties can be large for charm, relatively small for bottom